612-752 : 534. 015

Vibration of Air Suspension Bogies and Their Design*

By Naoteru ODA** and Seiichi NISHIMURA***

In this paper, at first the authors analyze the dynamic characteristics of the self-damped air spring on the basis of the linear theory from the standpoint of the design of air suspension bogies. The equivalent mechanical model of the self-damped air spring is obtained, which is a kind of so-called elastically supported damper systems, and the relationship among the elements of the model and the design parameters of the air spring are given.

Then, using the mechanical model, both natural vibration and transient response of the air suspension bogie are analyzed numerically. As the result, it is shown that the natural frequency and the damping ratio of the self-damped air suspension bogie scarcely vary with the car body weight, and the self-damped air suspension can reduce the magnitude of the transient response compared with a conventional mechanical suspension with oil-dampers.

1. Introduction

It is well known that air springs are self-damping elements as well as spring elements The self-damping action in the air spring can be achieved by an orifice between the air spring and the auxiliary reservoir or by an orifice on a partition which divides the interior of the air spring, as shown in Fig. 1. Recently, the self-damping action of the air spring is widely adopted for air suspensions of railroad bogies.

Dynamic characteristics of the self-damped air spring were analyzed by M. Kunieda[1] and T. Fujii[2] et al. and were considerably clarified. The theoretical analyses, however, were confined to their forced steady state vibration on account of its complexity. The air flow through an orifice has non-linear characteristics and the frequency response of the air suspension system is varied with the amplitude as well as the frequency. Even though the flow characteristic is to be linear, a degree of the damping of the self-damped air spring cannot be expressed by a constant damping coefficient, which is possible in case of an oil-damper connected in parallel with a spring.

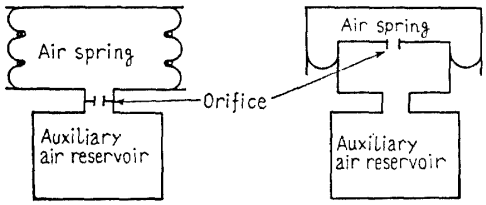

Fig. 1 Self-damped air spring with an orifice

* Received 21 st November, 1968.
** Assistant Manager, Central Research Laboratories, Sumitomo Metal Industries, Ltd., Amagasaki.
*** Research Engineer, Central Research Laboratories, Sumitomo Metal Industries, Ltd.

The results obtained by the authors on various kinds of air suspension bogies in service test showed that there existed a transient vibration rather than a forced one in the vibration of the bogies in service. Accordingly, the calculations of both the natural frequency and the degree of damping of the air suspension vehicle are required for the bogie design. Fortunately, the other test results[3] also showed that the pressure variation in the air springs and the auxiliary reservoirs had approximately linear characteristics for the vibration of the vehicle of low frequencies up to 2~3 Hz. Therefore, it is considered sufficient to analyze dynamic characteristics of an air spring on the linear vibration theory.

In the present paper, the authors attempt to represent the self-damped air spring by a simple mechanical model. The natural frequency and the degree of damping of the air suspension vehicle are calculated and also the transient response is analyzed. The design parameters of air springs are obtained in relation to the dynamic characteristics of the air suspension vehicles.

2. Linear spring characteristics and mechanical model Nomenclature

A_e: effective area

P_0, P_{at}: internal pressure at an equilibrium state and atmospheric pressure

P_a, P_b, p_a, p_b: internal pressures of the air spring

and the auxiliary reservoir, and their variances

V_a, V_b, v_a: internal volumes of the air spring and the auxiliary reservoir, and the variance of V_a

W_a, W_b, W_0: specific weights of the air in the air spring and the auxiliary reservoir, and their magnitude at the equilibrium state to static load

x: deflection of the air spring

n: polytropic index (n=1.4 for the calculation)

q: weight of the air passing through the orifice

$dq/dt>0$ if $p_a>p_b$

R: coefficient of flow resistance

Assuming that the air spring deflects from the equiliblium state and the internal pressure of the air spring varies according to the law of the polytropic change of air, the following equations are obtained for the air spring,

$$P_0V_a^n=P_a\left(V_a-v_a+\frac{q}{W_a}\right)^n \quad \cdots\cdots(1)$$

for the auxiliary reservoir

$$P_0V_b^n=P_b\left(V_b-\frac{q}{W_b}\right)^n \quad \cdots\cdots(2)$$

Neglecting the higher order terms of small quantities, they become

$$V_aW_0p_a+nP_0q=nP_0W_0v_a \quad \cdots\cdots(3)$$

$$V_bW_0p_b-nP_0q=0 \quad \cdots\cdots(4)$$

In case of the air spring, of which effective area scarcely varies with its deflection, it becomes approximately,

$$v_a=A_ex \quad \cdots\cdots(5)$$

When the characteristic of the air flow through the orifice is linear, it becomes

$$R\left(\frac{dq}{dt}\right)=p_a-p_b \quad \cdots\cdots(6)$$

Since the spring force of the air spring, F, is given by

$$F=A_e(P_0+p_a-P_{at})+(P_0-P_{at})\frac{dA_e}{dx}x \quad \cdots\cdots(7)$$

the following equations are obtained by eliminating q, P_a and v_a from Eqs. (3)~(6),

$$F=A_e(P_0-P_{at})+nA_e^2\frac{P_0}{V_a}x+(P_0-P_{at})\frac{dA_e}{dx}x-A_e\frac{V_b}{V_a}p_b \quad \cdots\cdots(8)$$

$$A_eR\frac{V_b}{n}\frac{W_0}{P_0}\frac{dp_b}{dt}+A_e\left(1+\frac{V_b}{V_a}\right)=n\frac{P_0}{V_a}A_e^2x \quad \cdots(9)$$

Putting $\frac{A_e}{\lambda k_1}p_b=y$, Eqs. (8) and (9) can be rewritten as follows,

$$F=F_0+k_2x+k_1(x-y) \quad \cdots\cdots(10)$$

$$c\dot{y}+\lambda k_1y=k_1(x-y) \quad \cdots\cdots(11)$$

where

$$\left.\begin{aligned} &k_1=nA_e^2\frac{P_0}{V_a},\quad k_2=(P_0-P_{at})\frac{dA_e}{dx}\\ &c=RA_e^2W_0,\quad \lambda=\frac{V_a}{V_b},\quad F_0=A_e(P_0-P_{at})\end{aligned}\right\}\cdots(12)$$

Equation (10) and (11) can be represented by the mechanical model as shown in Fig. 2, and the elements of the mechanical model can be related with the design parameters of the air spring by (12). In the mechanical model, an air spring having internal volume V_b and effective area A_e is connected in parallel with a dashpot, the damping coefficient of which is $RA_e^2W_0$, and an air spring having internal volume V_a and effective area A_e is connected in series with the parallel elements, and finally a spring, k_2, is installed in parallel with these three elements. The mechanical model shown in Fig. 2 is a kind of so-called elastically supported damper systems and it slightly differs from the model suggested by Murata[4] et al.

3. Natural frequency and damping of the air suspension system

Since, in case of the railroad bogies equipped with air springs, the stiffness of secondary suspension is much lower than that of primary suspension, the fundamental vibration in the vertical direction can be regarded as a single-degree-of-freedom vibration system.

As F_0 is equal to car body weight per an air spring, w, the equations of motion for free vibration can be expressed from Eqs. (10) and (11) as

$$\left.\begin{aligned} &\frac{w}{g}\ddot{x}+(k_1+k_2)x-k_1y=0\\ &c\dot{y}+(1+\lambda)k_1y=k_1x\end{aligned}\right\}\cdots\cdots(13)$$

where g is gravitational acceleration. Eliminating y in Eqs. (13) gives

$$\frac{w}{g}\ddot{x}+\frac{wk_1}{gc}(1+\lambda)\ddot{x}+(k_1+k_2)\dot{x}+\frac{k_1}{c}(\lambda k_1+\lambda k_2+k_2)x=0 \quad \cdots\cdots(14)$$

The following frequency equation can be obtained

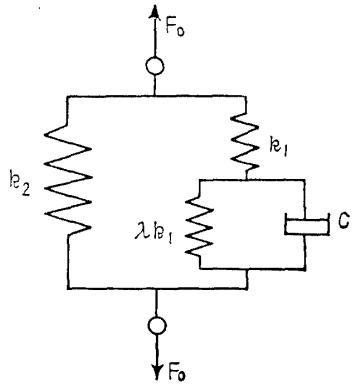

Fig. 2 Mechanical model of the self-damped air spring

from Eq. (14),

$$\mu^3+\frac{k_1}{c}(1+\lambda)\mu^2+\frac{g}{w}(k_1+k_2)\mu + \frac{k_1}{c}\frac{g}{w}(\lambda k_1+\lambda k_2+k_2)=0 \cdots\cdots\cdots(15)$$

If k_1 is not extremely large, Eq. (15) has two sets of solution; one is a non-vibratory solution, $\mu=-\mu_R$, and the other is a vibratory solution with damping, $\mu=-\mu_{cR}\pm i\mu_{cI}$, where μ_R, μ_{cR} and μ_{cI} are positive real numbers and $i^2=-1$.

At first, damped vibratory solutions, $\mu=-\mu_{cR}\pm i\mu_{cI}$, will be taken. In case of a single-degree-of-freedom system with spring and dashpot connected in parallel, the solution of the frequency equation can be expressed as $\mu=-h\omega_0\pm i\sqrt{1-h^2}\omega_0$, where ω_0 is the angular natural frequency and h the damping ratio.

Compared this solution with that of Eq. (15), the following relations are given,

$$\left.\begin{aligned}\omega_0&=2\pi f_0=\sqrt{\mu_{cI}{}^2+\mu_{cR}}\\ h&=\frac{\mu_{cR}}{\sqrt{\mu_{cI}{}^2+\mu_{cR}{}^2}}\end{aligned}\right\}\cdots\cdots\cdots(16)$$

f_0 and h obtained are denoted as natural frequency and damping ratio of the air suspension system, respectively. The relations between these quantities and design parameters of air springs will be discussed numerically in the following section.

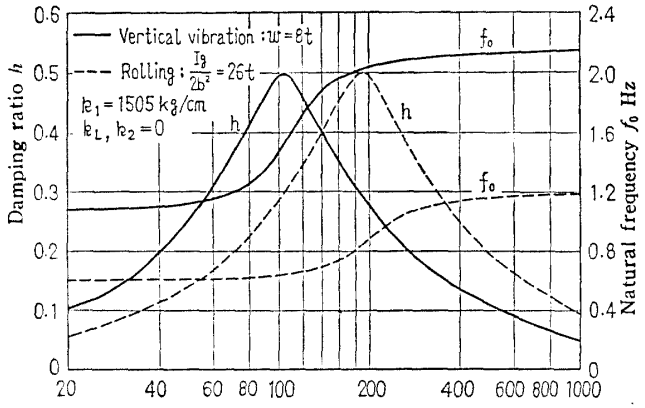

Fig. 3 Relations between h and c and between f_0 and c

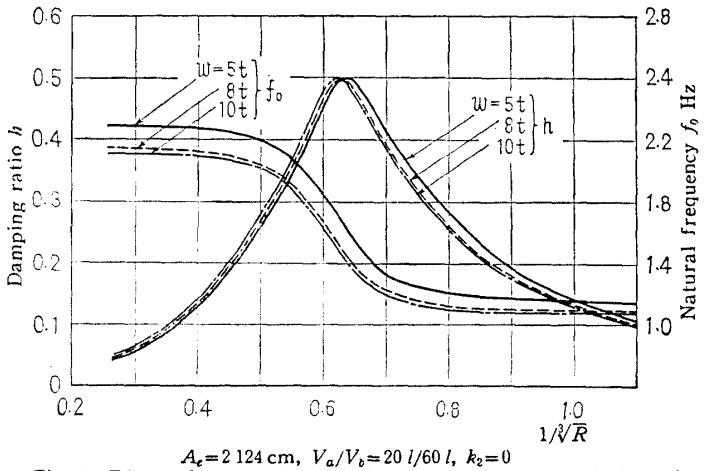

$A_e=2\,124$ cm, $V_a/V_b=20\ l/60\ l$, $k_2=0$

Fig. 4 Effect of the car body weight on the characteristics of vertical vibration

4. Results of numerical analysis

Taking appropriate values of w, k_1, k_2, and λ in Eq. (15), the relations between both c and w_0, and c and h can be calculated and are shown in Fig. 3.

It is seen from the mechanical model that f_0 is equal to $\frac{1}{2\pi}\sqrt{\left(\frac{\lambda}{1+\lambda}k_1+k_2\right)g/w}$ at $c=0$, then increases with c and finally tends to $\frac{1}{2\pi}\sqrt{(k_1+k_2)g/w}$ when $c=\infty$. On the other hand h has the maximum value at a certain value of c.

4·1 Effect of car body weight

Air pressure (P_0-P_{at}) is proportional to the car body weight. Since k_2 is proportional to (P_0-P_{at}) and k_1 is to P_0 as shown in (12), the ratio of stiffness of the air spring to the car body weight is kept almost constant. This is one of the well known characteristics of the air suspension system. The damping coefficient of the dashpot, c, in the mechanical model is also proportional to the specific weight of air, w_0, which is proportional to P_0 so that c also increases proportionally with the increase of the car body weight.

Consequently, the natural frequency and the damping ratio are approximately kept constant though the car body weight varies as shown in Fig. 4. Meanwhile, $1/\sqrt{R}$, which is proportional to the diameter of the orifice, is taken as the abscissa in Fig. 4 instead of c. From these considerations, the following numerical analyses are carried out for constant car body weight, 8 ton.

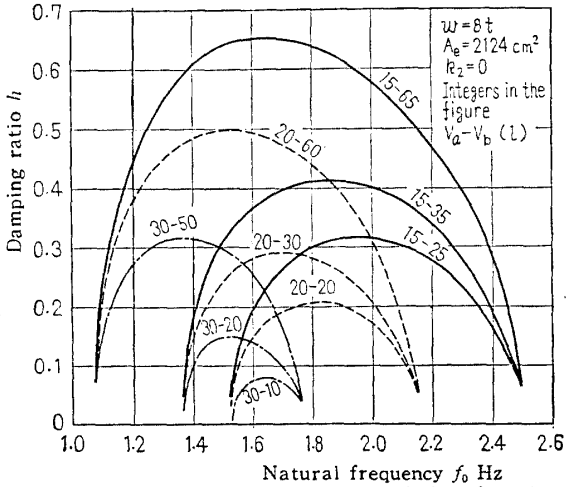

Fig. 5 Relation between the characteristics of vertical vibration and the tota volume of the air spring

4·2 Relation between volumetric ratio, λ, and total stiffness, $\frac{\lambda}{1+\lambda}k_1$

The relations between f_0 and h are depicted in Fig. 5 for given sets of k_1 and λ. The figure shows that h_{max}, the maximum value of h, increases when λ decreases and f_0 at h_{max} decreases as the total stiffness, $\frac{\lambda}{1+\lambda}k_1$, lowers. Accordingly, when the larger total volume of air spring, V_a+V_b, and the smaller ratio of λ are taken, the lower natural frequency and the larger damping action can be achieved.

4·3 Effect of k_2

The relations between f_0 and h for the given sets of k_2 and λ under the condition of the constant total stiffness, $\frac{\lambda}{1+\lambda}k_1+k_2$, and the constant k_1 are shown in Fig. 6. When k_2 changes from negative value to positive one, f_0 at h_{max} increases, and also magnitude of h_{max} becomes larger. The total volume of the air spring, however, rapidly increases as k_2 becomes positive, as shown in Fig. 7. This means that large damping can be obtained without varying f_0 if large total air volume is allowed and positive k_2 is taken. But, if an air spring of positive k_2 is adopted and, on the other hand, the total air volume is limited in a bogie design, f_0 becomes higher and, on the contrary, h_{max} becomes smaller so that the vibration characteristics become worse. The positive k_2 is not recommended.

In case of $k_2<0$, the required low value of f_0 can be obtained without large air reservoir but h_{max} decreases, so that sufficient damping action is hardly obtained. As the result, in order to give good vibration characteristics to an air suspension bogie, recommended k_2 is nearly equal to zero.

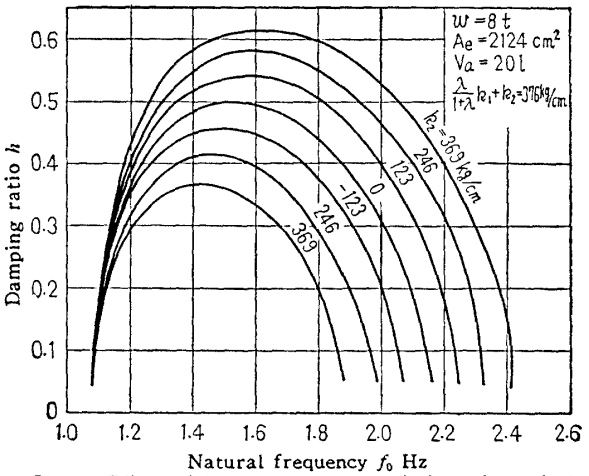

Fig. 6 Effect of k_2 on the characteristics of vertical vibration

4·4 Car body rolling

The riding quality of the vehicles is improved by using softer suspension, but the car body rolling (rolling about the lower longitudinal axis of the car body) becomes large and some difficulties are found in the bogie design. Therefore, in determining optimum design parameters of the bogie, the rolling as well as the vertical vibration has to be taken into consideration.

As far as the car body rolling is concerned, the motion can be expressed as a single-degree-of-freedom system as shown in Fig. 8.

The equations of motion are

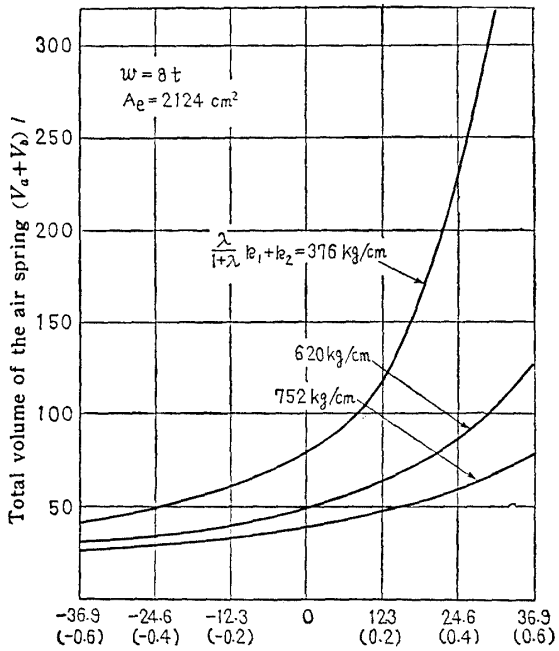

Fig. 7 Total volume of the air spring required for keeping a constant total stiffness when k_2 is varied

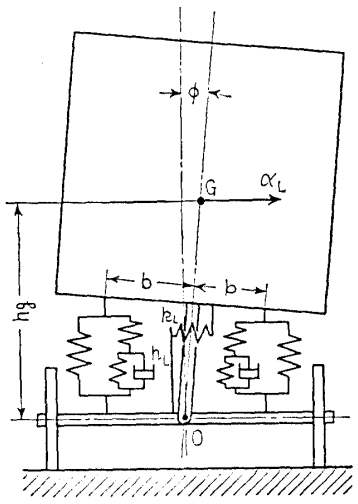

Fig. 8 Mechanical model of the car body rolling about lower longitudinal axis

$$\left.\begin{aligned} &I\ddot{\phi}+(k_L h_L^2-wh_g+2k_2b^2)\phi+2bk_1(b\phi-y)=0\\ &c\dot{y}+\lambda k_1 y=k_1(b\phi-y)\end{aligned}\right\} \quad \cdots\cdots(17)$$

where I is the moment of inertia of the car body about point 0.

The natural frequency and the damping ratio of the car body rolling, defined in the same manner as in the vertical vibration, can be calculated for the actual bogie $k_L h_L^2-wh_g \fallingdotseq 0$ and $I/2b^2=3.25$ w/g. Using these values and the others which are the same values as in the vertical vibration in Fig. 3, the dynamic characteristics of the car body rolling are calculated, which are shown by the dotted line in Fig. 3.

As the equations of motion show, they have the same tendency as the vertical vibration, but the natural frequency f_0 is lower than that of the vertical vibration. As for the damping ratio, the value of dashpot, c, corresponding to the h_{max}, differs between the rolling and the vertical vibration, and the former is larger than the latter. This implies that the value of c corresponding to the h_{max} increases when the natural frequency decreases.

Accordingly, for the bogie in trouble with the rolling (which is also related to the track and the operating conditions), c should be determined from the standpoints of both dynamic characteristics of the car body rolling and the vertical vibration. In some cases, high damping action with large value of c is required for reducing the car body rolling, allowing f_0 of the vertical vibration to increase.

5. Non-vibratory solution and transient response

So far as the stational vibration is concerned, the non-vibratory solution of Eq. (15) shown as, $\mu=-\mu_R$, is negligible, but is not always negligible in case of the transient response, for example, the transient response of vehicles running through the straight track with varied level or the entrance and exit of curved tracks. The deflection of the air spring becomes so large in the latter case that attention should be paid.

Thus, the transient response of the car body rolling which is expressed as a single-degree-of-freedom system shown in Fig. 8 is analyzed, and the relation between the non-vibratory solution and the transient response is discussed as follows.

When the lateral acceleration, $\alpha_L f(t)$, is applied to the center of gravity of the car body, the equations of motion are derived from Eqs. (17) as

$$\left.\begin{aligned} &I\ddot{\phi}+(k_L+2b^2k_1)\phi-2bk_1y=\frac{w}{g}h_g\alpha_L f(t)\\ &c\dot{y}+(1+\lambda)k_1y=bk_1\phi\end{aligned}\right\} \quad \cdots\cdots(18)$$

where, $K_L=k_L h_L^2+2k_2b^2-wh_g$.

Let ϕ_{st} be a roll angle when a constant lateral acceleration, α_L, is statically applied and put $\Phi=\phi/\phi_{st}$ and $Y=y/b\phi_{st}$, then Eqs. (18) are rewritten as

$$\left.\begin{aligned} &\ddot{\Phi}+\left(\omega_\phi^2+\frac{1}{1+\lambda}\omega_{\phi'}^2\right)\Phi-\omega_{\phi'}^2Y=\omega_\phi^2 f(t)\\ &\dot{Y}+(1+\lambda)\kappa Y=\kappa\Phi\end{aligned}\right\} \quad \cdots\cdots(19)$$

where, $\omega_\phi^2=\left(K_L+2\frac{\lambda}{1+\lambda}k_1b^2\right)\Big/I$, $\omega_{\phi'}^2=2k_1b^2/I$

and $\kappa=k_1/c$

5·1 Response to the lateral acceleration of a single rectangular pulse

Transient curves are generally provided at the entrance and exit of curved tracks, and their radii of curvature vary continuously between the straight track and the circular curved one. The lateral acceleration applied to a vehicle on curved tracks varies as shown in Fig. 9 (a), but sudden variation of the lateral acceleration, shown in Fig. 9 (b), occurs where the transient curve is not sufficient or is not provided in such a place as a rail point.

The analysis is carried out only for the worst condition, wherein the lateral acceleration is a single rectangular pulse as shown in Fig. 9 (b). The transient response becomes

$$\Phi=\begin{cases}\Phi_1(t) & t\leqq\tau\\ \Phi_1(t)-\Phi_1(t-\tau) & t>\tau\end{cases} \quad \cdots\cdots(20)$$

where,

$$\Phi_1=1-\omega_\phi^2\{D_1e^{-\mu_R t}+D_2e^{-\mu_{cR}t}\cos(\mu_{cI}-\psi)\}$$

$$D_1=\frac{\kappa(1+\lambda)-\mu_R}{\mu_R(\mu_R^2+\mu_{cR}^2+\mu_{cI}^2-2\mu_{cR}\mu_R)}$$

$$D_2=\sqrt{D_3^2+\frac{1}{\mu_{cI}^2}(D_4-\mu_{cR}D_3)^2}$$

$$D_3=\frac{\mu_{cR}^2+\mu_{cI}^2+\kappa(1+\lambda)(\mu_R^2-2\mu_{cR})}{(\mu_{cR}^2+\mu_{cI}^2)(\mu_R^2+\mu_{cR}^2+\mu_{cI}^2-2\mu_R\mu_{cR})}$$

$$D_4=\frac{\left[\begin{aligned}&(\mu_{cR}^2+\mu_{cI}^2)(\mu_R-2\mu_{cR})\\ &+\kappa(1+\lambda)(3\mu_{cR}^2-\mu_{cI}^2-2\mu_R\mu_{cR})\end{aligned}\right]}{(\mu_{cR}^2+\mu_{cI}^2)(\mu_R^2+\mu_{cR}^2+\mu_{cI}^2-2\mu_R\mu_{cR})}$$

$$\tan\psi=\frac{\mu_{cR}-(D_4/D_3)}{\mu_{cI}}$$

and μ_R, μ_{cR} and μ_{cI} are the roots of the frequency equation for the car body rolling.

Now, putting $Ig/2b^2=26$ t, $wh_g=8$ t·m, $k_1=1\,505$

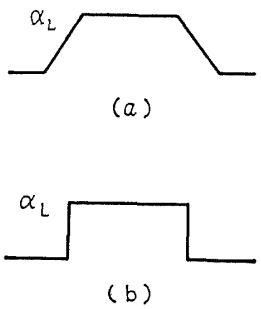

Fig. 9 Lateral acceleration applied to the car body on curved tracks

kg/cm and $k_L=0$, then, the transient responses are calculated by the analogue computer for (I) $\lambda=1/3$ and (II) $\lambda=2/3$.

Figure 10 shows two examples of the transient response. Figure 10 (a) is the transient response for the case of slight damping and Fig. 10 (b) is one for small κ as well as slight damping Fig. 10 where κ is smaller than that h_{max}. Fig. 10 (b) is the typical example where the non-vibratory solution has an important effect upon the transient response.

Transient responses are computed for a set of τ and the transient response spectrum[5] of Φ_{max} is obtained as shown in Fig. 11. In Fig. 11, a curve (III) is the transient response spectrum of a conventional vehicle which is suspended by a spring and an oil-damper. The damping ratios of the conventional vehicle have the same values as in the cases of (I) and (II). T in Fig. 11 is the natural period of the car body rolling without damping.

Figure 11 shows that difference in the transient responses among (I), (II), and (III) is negligibly

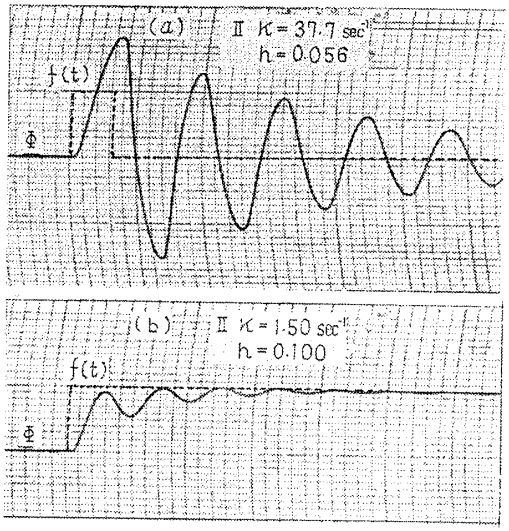

Fig. 10 Examples of the transient response for a single rectangular pulse

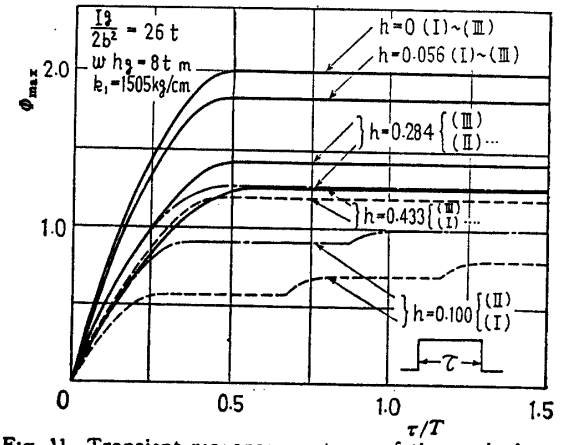

Fig. 11 Transient response spectrum of the car body rolling for a single rectangular pulse

small in case of comparatively small damping of $h=0.056$. It means that in case of small damping the maximum deflection of the spring in the transient response is proportional to the static deflection and does not depend on the damping mechanism.

As damping ratio increases and therefore κ decreases, the transient responses of (I) and (II) become smaller than that of (III) as shown in the figure in case of $h=0.284$ and $h=0.433$. However, it is difficult to make a general quantitative comparison, since the curve of transient response varies with λ and κ or ω_ϕ and $\omega_{\phi'}$. The reason why the transient response of (I) is larger than that of (III) for $\tau/T<0.5$ in case of $h=0.433$ is considered as follows. When a sudden change of applied force is imposed on the vehicle, the frequency of the response becomes higher than the natural frequency. On the other hand, $h=0.433$ corresponds to h_{max} of (I). As the result, the degree of damping of the case (I) is substantially decreased, and the transient response curves of (I) and (III) are reversed for $\tau/T<0.5$.

Next, for small κ beyond h_{max}, Φ_{max} of the second cycle becomes larger than the first cycle in some cases, shown in Fig. 10 (b). This occurs when the non-vibratory solution, μ_R, is comparatively small and $e^{-\mu_R t}$ in Φ_1 of Eq. (20) cannot be neglected. Figure 12 shows relations between h and μ_R. In the figure μ_R increases with h in the first stage and h reaches its maximum value, whereas the rate of increase of μ_R becomes greater as λ increases. In case of the same damping ratio, number of cycles

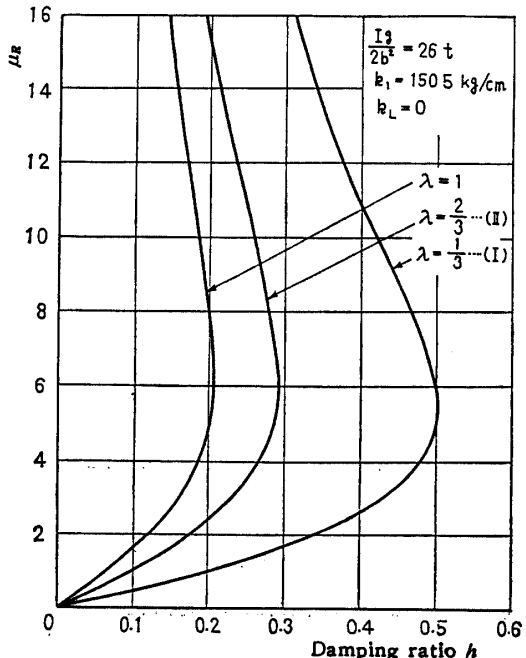

Fig. 12 Relation between h and μ_R when the volumetric ratio, λ, is varied

required for Φ_{max} reaching near a unit angle increases with the decrease of λ as shown in (I) and (II) of $h=0.1$ in Fig. 11.

The results mentioned above mean that in order to reduce the deflection of the suspension spring in transient response, the suspension of the self-damped air spring is more advantageous than that of a spring and an oil damper connected in parallel. Use of an orifice of small diameter is effective to get more reduction of the spring deflection only for short duration of time.

5·2 Response to the lateral acceleration of a full-cycle of rectangular pulse

When a vehicle runs through S curved track or moves from one truck to an adjacent truck, the inverse acceleration is applied moreover. The transient response in this case is computed in a similar way to the previous section for the case (II). Figure 13 shows two examples of the transient response for the acceleration of a full-cycle rectangular pulse. Figure 13 (a) shows the transient response in the state of resonance for a slight damped system, and Fig. 13 (b) is an example for small κ. The transient response spectrum in this case is shown in Fig. 14. It shows that the maximum value of the transient response for a full-cycle rectangular pulse is affected by the frequency of the acceleration if damping is small, but for the larger damping ratio such as $h=0.284$, the effect of the frequency is reduced. Consequently, the maximum value of the transient response for a full-cycle rectangular pulse is considered to be nearly equal to that for a single rectangular pulse.

6. Conclusions

(1) The self-damped air spring with an orifice has the same dynamic characteristics as the elastically supported damper system when the characteristic of the air flow through the orifice is assumed to be linear. In the mechanical model, an air spring having internal volume V_b and effective area A_e is connected in parallel with a dashpot, the damping coefficient of which is $RA_e^2W_0$, and an air spring having internal volume V_a and effective area A_e is connected in series with the parallel elements, and finally a spring, k_2, is installed in parallel with these three elements.

(2) The natural frequency and the damping ratio of the self-damped air suspension bogie scarcely vary with the car body weight, since the stiffness of the springs and the coefficient of damping of the dashpot in the mechanical model are approximately proportional to the car body weight.

(3) In order to lower the natural frequency and to raise the damping ratio, it is effective to adopt not only a larger total volume of the air spring but also a smaller volumetric ratio of the air spring to the auxiliary air reservoir. However, the requirement for reducing the total volume of the air spring without a change of the dynamic characteristics is satisfied when $k_2=0$.

(4) The magnitude of transient response of the air suspension bogie is generally smaller than that of the suspension system in which a spring and an oil-damper are connected in parallel, and this characteristic is advantageous for the bogie design.

Acknowledgment

The authors express their gratitude to Prof. H. Tokumaru, Faculty of Engineering, Kyoto University for his valuable advice and useful discussion. The authors also express their gratitude to Dr. M. Sumitomo, Manager, and Dr. K. Nishioka, Senior Research Engineer, of Central Research Laboratories, Sumitomo Metal Ind., Ltd., for their support and encouragement.

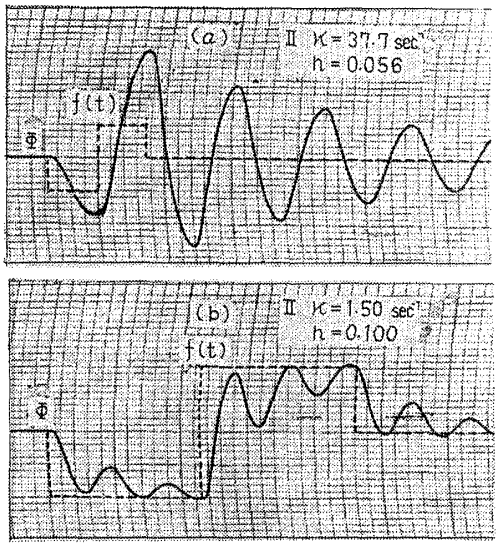

Fig. 13 Examples of the transient response for a full-cycle of rectangular pulse

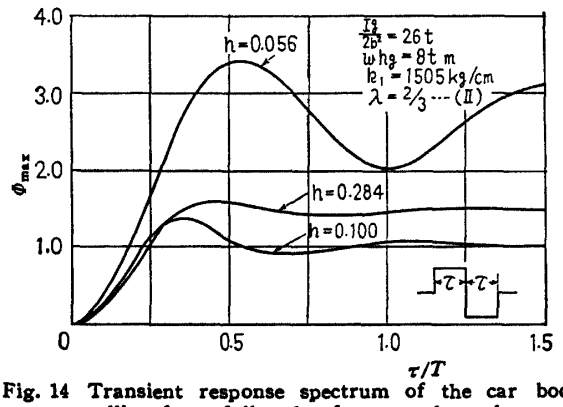

Fig. 14 Transient response spectrum of the car body rolling for a full-cycle of rectangular pulse

References

(1) M. Kunieda: *Railw. Tech. Research Report*, No. 6 (1958).
(2) T. Fujii et al.: *Air spring*, (1961), p. 119, Nikkankogyo Press.
(3) N. Oda et al.: *Sumitomo Metal*, Vol. 16, No. 3 (1964), p. 41.
(4) N. Murata et al.: *Hitachi Hyoron*, Vol. 39, No. 2 (1957), p. 74.
(5) L. S. Jacobsen and R. S. Ayre: *Engineering Vibrations*, (1958), p. 160, McGraw-Hill.